1953-10

A Study of Constant Absolute Vorticity Trajectories on Isentropic Surfaces

Carlstead, Edward M.

Journal of Meteorology. Volume 10 (October 1953); p. 356-361
https://hdl.handle.net/10945/48909

A STUDY OF CONSTANT ABSOLUTE VORTICITY TRAJECTORIES ON ISENTROPIC SURFACES

By LT Edward M. Carlstead, U.S.N.

U. S. Naval Postgraduate School [1,2]

(Manuscript received 17 February 1953)

ABSTRACT

It is shown that constant absolute vorticity (CAV) trajectories are more useful on isentropic surfaces than on constant pressure surfaces. A form of the vorticity equation is derived by use of Lagrangian methods. This form is similar to the Rossby form, and ordinary methods of computing CAV trajectories can be used with isentropic charts.

A series of isentropic streamline charts was prepared and CAV trajectories were constructed at certain points on these charts. CAV trajectories were also constructed on 500-mb charts for the same time. 24- and 48-hr forecasts of wind direction and speed were made from CAV trajectories on both sets of charts, and verified. The results of these forecasts are treated statistically, and forecasts from CAV trajectories on isentropic charts are shown to be significantly better than similar forecasts from 500-mb charts.

The effects of the divergence term of the vorticity equation are discussed qualitatively.

1. Introduction

The meteorologist is often called upon to forecast for periods in excess of 24 hr, a task for which simple extrapolation is generally insufficient. One method of forecasting entails preparation of prognostic surface charts and preparation of forecasts from these charts. As most meteorologists know, this is easier said than done. One of the important tools used in estimating the future position and intensity of surface systems is a prognostic 500-mb chart. At present, much attention is being paid to methods for preparing such charts, and one of the techniques used is the construction of forecast air-parcel trajectories, based on the principle of conservatism of the vertical component of absolute vorticity, $\zeta + f$. Here ζ is the vertical component of relative vorticity and f is the Coriolis parameter. Rossby [8] initiated the vorticity concept by showing that under certain restrictive assumptions, the following relationship holds:

$$\zeta + f = \text{constant}.$$

The assumptions referred to above are as follows:

1. The atmosphere is a homogeneous, incompressible fluid;
2. Motion is purely horizontal;
3. Friction forces are neglected; and
4. There is no horizontal divergence.

Rossby [9] then integrated his fundamental equation, and was able to obtain trajectories for particles which conserve their vertical component of absolute vorticity. These are known as constant absolute vorticity trajectories, and will be referred to as CAV trajectories.

The assumptions necessary to derive the vorticity equation as Rossby did are quite restrictive. Shaw [10] first suggested that charts of isentropic surfaces should be drawn, as motion of air is best resolved on these surfaces. Namias [6] states that, from available observations, isentropic surfaces appear to be substantial surfaces (*i.e.*, surfaces that contain the same particles from day to day), to a first approximation. Starr [11] suggested that CAV trajectories might better be depicted on an isentropic chart than on a constant level chart, as there are no solenoids on isentropic surfaces. It would then seem that the technique of forecasting future positions of particles by CAV trajectories would be best applied to isentropic surfaces. It will be shown in this paper that the prognostic trajectory based on the conservatism of the vertical component of absolute vorticity is theoretically and practically better suited to use on isentropic charts, than on constant pressure charts where it is now applied.

2. Theoretical investigation

The derivation of a vorticity equation for flow on an isentropic surface requires fewer assumptions than does the derivation for constant level surfaces. The motion of particles on a substantial surface can be described with Lagrangian methods. The particular derivation of the vorticity equation presented here is due to Haltiner.

Let x, y, z and t be normal Cartesian coordinates, and let X, Y, Z and τ be Lagrangian coordinates, where X and Y are coordinates of the horizontal pro-

[1] Present address: U.S.S. Curtiss (AV-4).

[2] Part of a thesis submitted to the Department of Meteorology, U. S. Naval Postgraduate School, in partial fulfillment of the requirements for the degree of Master of Science.

jection of the isentropic surface, $Z = z$, and τ refers to time for the isentropic surface. Then

$$\frac{\partial p}{\partial X} = \frac{\partial p}{\partial x} + \frac{\partial p}{\partial z}\frac{\partial z}{\partial X} = \frac{\partial p}{\partial x} - g\rho\frac{\partial z}{\partial X},$$

$$\frac{\partial p}{\partial Y} = \frac{\partial p}{\partial y} + \frac{\partial p}{\partial z}\frac{\partial z}{\partial Y} = \frac{\partial p}{\partial y} - g\rho\frac{\partial z}{\partial Y}.$$

It follows from the above equations that

$$-\rho^{-1}\partial p/\partial x = -\partial F/\partial X \tag{1}$$

and

$$-\rho^{-1}\partial p/\partial y = -\partial F/\partial Y, \tag{2}$$

where $F = c_pT + gz$, the stream function for an isentropic surface. In a similar way we find

$$\frac{\partial u}{\partial x} = \frac{\partial u}{\partial X} - \frac{\partial u}{\partial z}\frac{\partial z}{\partial X}, \quad \frac{\partial v}{\partial x} = \frac{\partial v}{\partial X} - \frac{\partial v}{\partial z}\frac{\partial z}{\partial X},$$
$$\frac{\partial u}{\partial y} = \frac{\partial u}{\partial Y} - \frac{\partial u}{\partial z}\frac{\partial z}{\partial Y}, \quad \frac{\partial v}{\partial y} = \frac{\partial v}{\partial Y} - \frac{\partial v}{\partial z}\frac{\partial z}{\partial Y}, \tag{3}$$

and

$$\frac{\partial u}{\partial \tau} = \frac{\partial u}{\partial t} + \frac{\partial u}{\partial z}\frac{\partial z}{\partial \tau}, \quad \frac{\partial v}{\partial \tau} = \frac{\partial v}{\partial t} + \frac{\partial v}{\partial z}\frac{\partial z}{\partial \tau}. \tag{4}$$

Further, since the motion is assumed adiabatic

$$w = \frac{\partial z}{\partial \tau} + u\frac{\partial z}{\partial X} + v\frac{\partial z}{\partial Y}. \tag{5}$$

Substituting in the equations of motion,

$$\frac{\partial u}{\partial t} + u\frac{\partial u}{\partial x} + v\frac{\partial u}{\partial y} + w\frac{\partial u}{\partial z} = -\rho^{-1}\frac{\partial p}{\partial x} + fv,$$
$$\frac{\partial v}{\partial t} + u\frac{\partial v}{\partial x} + v\frac{\partial v}{\partial y} + w\frac{\partial v}{\partial z} = -\rho^{-1}\frac{\partial p}{\partial y} - fu, \tag{6}$$

the expressions (1), (2), (3), (4) and (5), we obtain

$$\frac{\partial u}{\partial \tau} + u\frac{\partial u}{\partial X} + v\frac{\partial u}{\partial Y} = -\frac{\partial F}{\partial X} + fu, \tag{7}$$

and

$$\frac{\partial v}{\partial \tau} + u\frac{\partial v}{\partial X} + v\frac{\partial v}{\partial Y} = -\frac{\partial F}{\partial Y} - fu. \tag{8}$$

Differentiating (7) with respect to Y, and (8) with respect to X, subtracting and collecting terms, we obtain

$$-\frac{\partial}{\partial \tau}(\zeta_\theta) + \left(\frac{\partial v}{\partial Y} + \frac{\partial u}{\partial X}\right)\left(\frac{\partial u}{\partial Y} - \frac{\partial v}{\partial X}\right) + u\frac{\partial}{\partial X}\left(\frac{\partial u}{\partial Y} - \frac{\partial v}{\partial X}\right) + v\frac{\partial}{\partial Y}\left(\frac{\partial u}{\partial Y} - \frac{\partial v}{\partial X}\right) = u\frac{\partial f}{\partial X} + v\frac{\partial f}{\partial Y} + f\left(\frac{\partial u}{\partial X} + \frac{\partial v}{\partial Y}\right).$$

In vector notation, this becomes

$$-[\partial/\partial\tau(\zeta_\theta) + V\cdot\nabla_{2\theta}\zeta_\theta] - \zeta_\theta\nabla_{2\theta}\cdot V = V\cdot\nabla_{2\theta}f + f\nabla_{2\theta}\cdot V + \partial f/\partial\tau,$$

where the operator

$$\nabla_{2\theta} = i(\partial/\partial X) + j(\partial/\partial Y).$$

Finally, we may write this as

$$d(\zeta_\theta + f)/dt + (\zeta_\theta + f)\nabla_{2\theta}\cdot V = 0, \tag{9}$$

since $\tau = t$ for any particle. Now, assume the divergence term $\nabla_{2\theta}\cdot V$ to be zero. Then we may write (9) in the familiar form

$$d(\zeta_\theta + f)/dt = 0, \tag{10}$$

or

$$\zeta_\theta + f = \text{constant}.$$

While this form is similar to the form derived by Rossby, there are some fundamental differences. Parcel motion is not limited to the horizontal plane, but is three dimensional. Moreover, an incompressible atmosphere is not required.

3. Technique of investigation

The vertical component of relative vorticity may be written in the form

$$\zeta_\theta = V/R_s - \partial V/\partial N,$$

where R_s is the radius of curvature of a streamline measured on the isentropic chart, and N is the direction normal to the streamline on the isentropic chart. If we select a parcel in a broad uniform flow or in the axis of the jet stream, $\partial V/\partial N = 0$. Further, if the parcel is at an inflection point in the flow, $V/R_s = 0$. Under these conditions, where $\zeta_\theta = 0$, a CAV trajectory can be computed. It will be noted that R_s, defined above, is not exactly equal to the projected radius of curvature of a streamline on an isentropic surface. However, the error due to this approximation is normally less than those made in the actual computation of CAV trajectories as described by Fultz [4] and revised by Wobus [13].

The simplest method of obtaining a CAV trajectory is through the use of a mechanical device such as the so-called "wiggle-wagon" devised by Wobus [13], and currently in use in the U. S. Weather Bureau-Air Force-Navy Analysis Center, Washington, D. C. The prime advantage of the "wiggle-wagon" is that it rapidly computes trajectories for a spherical earth, instead of for a plane earth which most previous techniques assumed. The U. S. Navy's Project AROWA [12] has published a table for computing CAV trajectories made from trajectories traced by the "wiggle-wagon." This table is used to compute CAV trajectories in this paper.

The next step in the investigation was to compute trajectories on isentropic and 500-mb charts, and test the results statistically.

A rather complete compilation of upper air and surface data is available in the *Northern hemisphere surface and 500 millibar charts series*, published by the U. S. Weather Bureau. Data were taken from the period of January–February 1949. From these data, a set of thirty isentropic charts was plotted. The 303-K isentropic surface was selected because (1) this surface was often close to the so-called "level of non-divergence" [1], (2) this surface often contained much of the 500-mb wind-speed maximum axis (jet), and (3) the 303-K isentropic surface was usually sufficiently far from the surface to be free from effects of surface friction and turbulence. It was desired to select an isentropic surface containing much of the 500-mb isotach-maximum axis (jet), so computation of CAV trajectories could aid in the prognosis of the 500-mb surface. Inasmuch as the derivation of CAV trajectories on an isentropic surface assumes the divergence term to be zero, the selection of a surface close to the level of non-divergence is desirable. The effect of the divergence term is discussed in the next section.

After the heights of the 303-K isentropic surface were plotted, all available wind data pertinent to the isentropic surface were plotted. Where wind observations were available from pibal stations not having radiosonde observations, an interpolated value of the height of the isentropic surface and the wind nearest the interpolated height was entered on the chart. Because of the fairly dense network of upper wind observing stations in the United States, a sufficiently accurate streamline analysis was possible without the time-consuming computations of stream-function values.

Streamline analyses were made at 0300 GCT each day, in the period from 6 January 1949 to 22 January 1949, and from 10 February 1949 to 20 February 1949. For each chart, a number of CAV trajectories was computed. The following conditions had to be met before choosing an initial inflection point for CAV trajectory computation: (1) the point had to be at or very near an inflection point in the flow (undergoing no effects of curvature), (2) the point had to be at or very near the axis of the isotach maximum (jet) or in a broad uniform flow, and (3) the point must be a wind-observation point to obtain the correct, initial wind speed and direction. This procedure netted from one to four points per chart, suitable for CAV-trajectory computation.

For comparison with each CAV trajectory plotted on the isentropic chart, a companion CAV trajectory was plotted on the 500-mb chart of the same time. It was not difficult to find a companion inflection point on the 500-mb chart, as the isentropic surface was usually close to the 500-mb surface. After CAV trajectories were plotted on both sets of charts, a forecast wind velocity was determined by moving the parcel along the forecast trajectory a distance equal to the product of the initial wind speed and the number of hours to forecast time. Selected forecast times were 24, 48 and 72 hr. All forecast wind velocities were verified where possible. On the isentropic charts, verification depended on the forecast wind position falling within the observational network. If, then, the forecast wind was not at a reporting station, the forecast wind was verified by linear interpolation between nearby stations. However, care was taken to use only stations where linear interpolation was reasonable. On the 500-mb chart, forecast winds were verified in

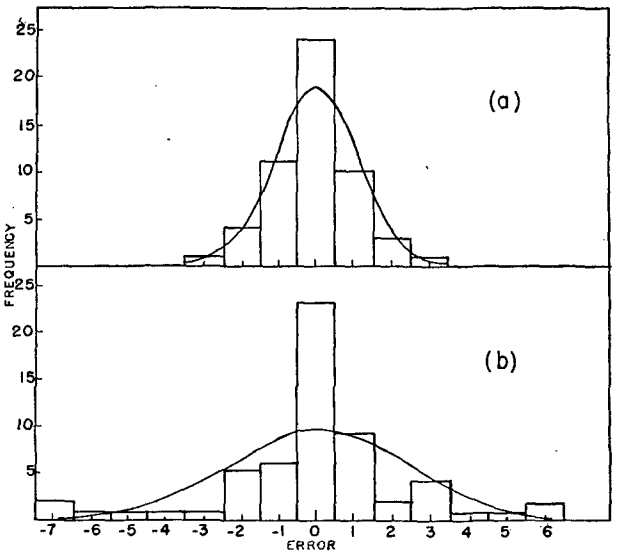

FIG. 1. Distribution of cases of 24-hr wind-direction error from (a) isentropic charts and (b) 500-mb charts. Error: tens of deg.

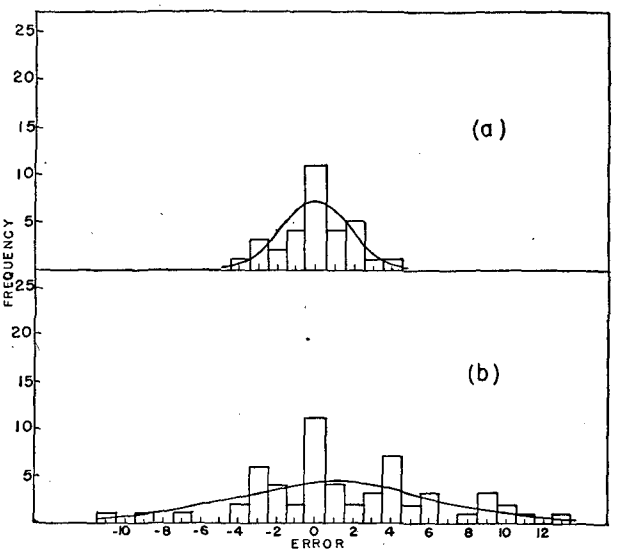

FIG. 2. Distribution of cases of 48-hr wind-direction error from (a) isentropic charts and (b) from 500-mb charts. Error: tens of deg.

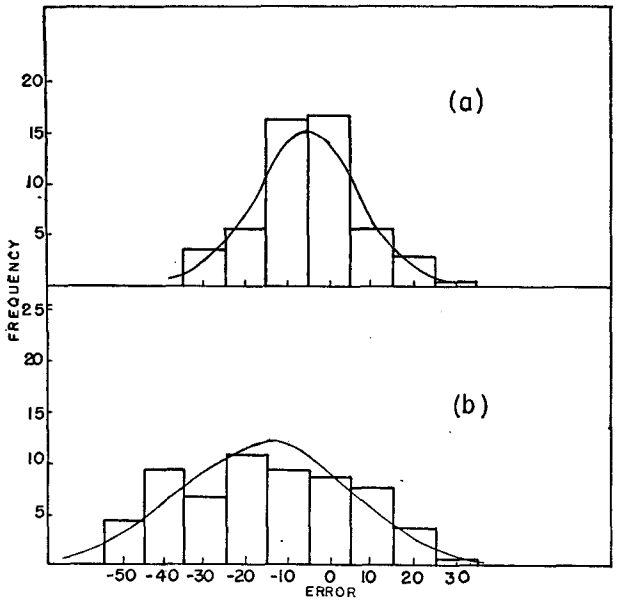

FIG. 3. Distribution of cases of 24-hr wind-speed error from (a) isentropic charts and (b) from 500-mb charts. Error: knots.

a similar manner, except that when the forecast wind velocity fell outside the observational network, contours were assumed to be streamlines, and gradient winds were measured for verification. Because verification on isentropic charts depended on wind velocities falling within the observational network, the number of verified forecasts dropped off drastically after 48 hours. However, with hemispherical 500-mb charts available, forecasts made on this surface could always be verified.

In the verification of forecast winds, a direction error was negative if the observed direction was to the right (clockwise) of the forecast direction, and positive if to the left of the forecast direction. Similarly, a wind-speed error was negative if the observed speed was less than the forecast speed, and positive if more than the forecast speed. All forecast winds and verifications were tabulated in a form suitable for statistical testing.

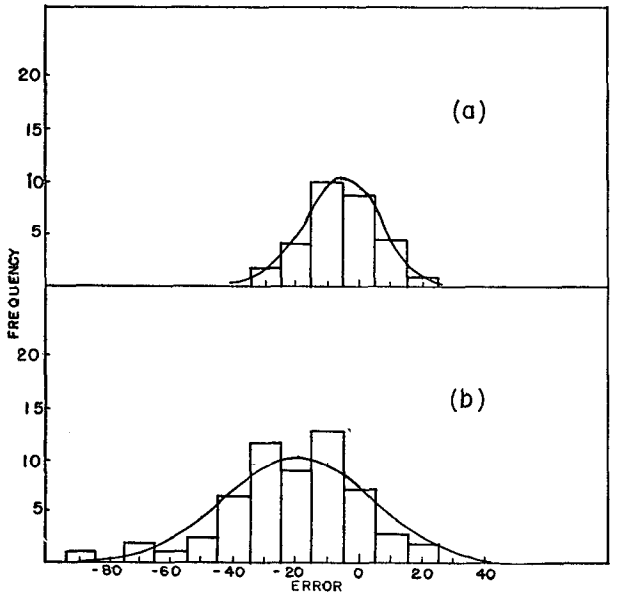

FIG. 4. Distribution of cases of 48-hr wind-speed error from (a) isentropic charts and (b) from 500-mb charts. Error: knots.

Histograms of wind-speed error and wind-direction error were prepared for 24- and 48-hr forecast times, for both the isentropic and 500-mb charts. These histograms are shown in figs. 1 through 4. Wind-speed errors were grouped into cells; each having an interval of 10 kn, with cell midpoints at 0, ± 10, ± 20, *etc.*, knots. All wind-direction errors were recorded in increments of 10 deg, with cell midpoints at 0, ± 10, ± 20, *etc.*, degrees.

Normal curves were fitted to the data in the histograms, in accordance with the method described by Hoel [5, pp. 191–194]. Then χ^2 tests were performed, and it was found that, in all cases, the data could reasonably be said to have come from a normal parent population. The distributions of data from the isentropic charts were then compared with similar distributions of data from the 500-mb charts, by use of the F test, to determine if the distributions could be from the same normal parent population. If the test were to show that there is a significant difference between data from the isentropic charts and from the 500-mb charts, a decision could be made as to which of the two types of charts is better suited to forecasts of CAV trajectories.

4. Results

It was found that 24-hr forecasts of wind directions were within ± 20 deg of observed directions in 96.4 per cent of the cases from isentropic charts, and in 76.3 per cent of the cases from 500-mb charts. Percentages are 81 and 41 respectively, for 48-hr direction forecasts.

The 24-hr forecasts of wind speed were within ± 15 knots of observed speeds in 76 per cent of the cases from isentropic charts, and in 42.4 per cent of the cases from 500-mb charts. Percentages are 78.5 and 39 respectively, for 48-hr wind-speed forecasts. Thus, superior wind forecasts, by means of CAV trajectories, were obtained on isentropic charts during the period of this study.

The F test [5, pp. 152–154] is a statistical test for comparing variances (s^2) of two samples of data, to determine if they reasonably belong to the same normal population of data. The basic requirement of the F test is that the samples must be from normal populations, although not necessarily the same normal population. This is why it was necessary to show normality of the data samples. The F test is applied by assuming there is no significant difference between the samples tested (the null hypothesis). If the value of

F computed is above a critical value, we assume there is a significant difference between the samples (the null hypothesis is denied), and the samples do not reasonably belong to the same parent normal population. It is this condition we wish to obtain. The results of the F test are as follows:

1. 24-hr wind-direction error. The variance of data from isentropic charts is 1.24; from 500-mb charts it is 6.37. Then $F = s_1^2/s_2^2 = 6.37/1.24 = 5.14$. F_c, at a 95 per cent level of belief, is 4.90. Therefore, the samples tested are significantly different. See fig. 1.
2. 48-hr wind-direction error. The variance of data from the isentropic charts is 3.15, that from the 500-mb charts is 30.75. Then $F = 9.75$. F_c, at a 95 per cent level of belief, is 3.75. This result is highly significant. See fig. 2.
3. 24-hr wind-speed error. The variance of data from the isentropic charts is 155.7; from the 500-mb charts it is 413.7. Then $F = 2.65$. F_c, at a 95 per cent level of belief, is 5.19, and there is no significant difference between the two samples of data. See fig. 3.
4. 48-hr wind-speed error. The variance of data from the isentropic charts is 127.3, that from the 500-mb chart is 515.5. Then $F = 4.05$. F_c, at a 90 per cent level of belief, is 4.00, and the results are significantly different. See fig. 4.

Significance was obtained in both cases of wind-direction error and in one case of wind-speed error. In each of the cases where significance was obtained, an examination of the data shows that it is the data from trajectories constructed on isentropic charts that are better.

It is gratifying to note that the greatest improvement was shown in the wind-direction forecasts for 48 hr. In much operational forecasting, wind direction is usually deemed more important than wind speed, since the proper location of troughs, ridges and associated weather patterns depends greatly on correct wind-direction forecasts. Therefore, from results obtained, the CAV trajectory method developed herein will show greatest improvement over the present system of taking CAV trajectories on constant pressure charts if used on isentropic charts to forecast wind direction, at least up to 48 hr.

In a recent study by Bruch [2] of CAV trajectories along a pseudo 600-mb surface, wind-direction errors are quite similar to those obtained here for 500-mb charts. Bruch did not verify wind speeds.

It is realized that the isentropic chart leaves much to be desired as an operational weather chart. At present, the chart is laborious to plot since no data are transmitted on teletype circuits; however, if such data were transmitted, streamline analysis would take little longer to prepare than would the present 500-mb chart. Another difficulty is that the movement of the isentropic surface is not easy to predict. Since any CAV trajectory, as developed here, is a two dimensional projection of a three dimensional path, the height of the parcel in the future is not certain unless the isentropic surface is stationary. A future study to relate this study with prognosis of the isentropic surface could be advantageous.

CAV trajectories on isentropic surfaces should be of great aid in locating troughs and ridges in flow patterns of nearby constant pressure surfaces. Also, since surface systems are related to flow patterns aloft, the correct forecasting of isentropic flow patterns will aid forecasts at the surface.

In one form of the vorticity equation, the divergence term is assumed to be zero. This assumption is not always fulfilled in the atmosphere where this term may be important. As an illustration, let the divergence term $\nabla_{2\theta} \cdot V$ be constant in (9), and integrate with respect to t to obtain

$$\zeta_\theta + f = c \exp\left[-(\nabla_{2\theta} \cdot V)\, \Delta t\right].$$

Let $t = 0$ at the initial inflection point, where $\zeta_\theta = 0$. Then

$$\zeta_\theta + f = c = f_0$$

and

$$\zeta_\theta = f_0 \exp\left[-(\nabla_{2\theta} \cdot V)\, \Delta t\right] - f. \qquad (11)$$

As can be seen, positive values of the divergence term in a northwesterly flow will cause a negative contribution to the vertical component of relative vorticity of a parcel, causing it to go farther south than would be indicated by a CAV trajectory. Positive values of the divergence term in southwesterly flow will have a similar effect on the relative vorticity of a parcel, not permitting it to reach the maximum latitude of the CAV trajectory. Negative values of the divergence term will cause positive contributions to the relative vorticity of the parcel. In northwesterly flow, this will cause a parcel to curve more cyclonically than indicated by a CAV trajectory, and to curve less cyclonically in southwesterly flow. Fultz [4] mentions that at the 10,000-ft level, the average deviation from CAV trajectories could be caused by horizontal velocity divergence in northwesterly flow and convergence in southwesterly flow.

Now,

$$\nabla_{2\theta} \cdot V = \frac{\partial u}{\partial X} + \frac{\partial v}{\partial Y} = \left(\frac{\partial u}{\partial x} + \frac{\partial v}{\partial y}\right) + \left(\frac{\partial u}{\partial z}\frac{\partial z}{\partial X} + \frac{\partial v}{\partial z}\frac{\partial z}{\partial Y}\right).$$

Thus, the divergence term is composed of two parts, horizontal velocity divergence and a shear term. Fleagle [3] and Panofsky [8] have given several values for horizontal divergence, with a range of about $\pm 5 \times 10^{-6}$ sec^{-1}. Values of the shear term could be computed at initial inflection points for 34 of the CAV trajectories on isentropic charts in this study. In 14 cases the term was less than 10^{-7} sec^{-1}. In 11 cases the value of the shear term was approximately 10^{-6} sec^{-1},

and in 9 cases, approximately -10^{-6} sec^{-1}. Usually the shear term was positive or negative if the flow was up or down the isentropic surface, respectively. From this we see that in about 60 per cent of the cases studied, the shear term was of the same order of magnitude as the horizontal velocity divergence. In these cases, the shear term either nearly cancelled or doubled the horizontal velocity divergence. Now, if the assumption that $\nabla_{2\theta} \cdot V = 0$ were the most important assumption in the present development of CAV trajectories, we might expect forecasts of future positions of parcels by CAV trajectories to be in greater error, in some cases, on isentropic surfaces than on constant pressure surfaces. This was not observed in the data collected in this study. This may suggest that the assumption of no horizontal divergence is not too restrictive, and that possibly one of the other assumptions made by Rossby is more restrictive, such as the assumption of purely horizontal motion.

If we take a large constant value for horizontal velocity divergence, say 6×10^{-6} sec^{-1}, take a like value for the shear term, assume a time period of 12 hours, and use these values in (11), we would find that the value of f_0 at latitude 45 deg is reduced by 33 per cent, or to the value of f at latitude 33 deg. But this is an extreme case, and the effects of the divergence term are usually much less. However, since the assumption that $\nabla_{2\theta} \cdot V = 0$ does lead to error, further work would be desirable to correct the CAV-trajectory method for effects of the divergence term.

REFERENCES

1. Bjerknes, J., and J. Holmboe, 1944: On the theory of cyclones. *J. Meteor.*, **1**, 12–13.
2. Bruch, A., 1952: Verification of constant absolute vorticity trajectories. *Experiments in Qualitative Prediction with Aid of Upper Air Charts*. Chicago, Dept. Meteor., Univ. Chicago.
3. Fleagle, R., 1948: Quantitative prediction of factors influencing pressure changes. *J. Meteor.*, **5**, 281–292. (See p. 289.)
4. Fultz, D., 1944: Upper air trajectories and weather forecasting. Dept. Meteor., Univ. Chicago, *Miscellaneous Report* No. 19.
5. Hoel, P., 1947: *Introduction to mathematical statistics*. New York, Wiley and Son.
6. Namias, J., 1940: Isentropic analysis, in *Weather analysis and forecasting*, by S. Petterssen. New York, McGraw-Hill, 503 pp. (See pp. 372–374.)
7. Panofsky, H., 1949: Objective weather map analysis. *J. Meteor.*, **6**, 386–392.
8. Rossby, C.-G., 1939: Variations in intensity of zonal circulation of the atmosphere and displacement of the semi-permanent centers of action. *J. marine Res.*, **2**, 38–55.
9. ——, 1942: Forecasting of flow patterns in the free atmosphere by a trajectory method, in *Basic principles of weather forecasting*, by V P. Starr. New York, Harper Brothers, 299 pp.
10. Shaw, Sir N., 1933: *Manual of meteorology*, **3**. Cambridge, Cambridge University Press, 445 pp. (See p. 263.)
11. Starr, V. P., 1945: Comment by editor, *J. Meteor.*, **2**. (See p. 133.)
12. U. S. Navy, Bureau of Aeronautics, Project AROWA, 1952: *Topical outline of refresher course for reserve aerologists in recent developments in upper air analysis and forecasting*. Norfolk, Section 7.
13. Wobus, H. B., 1950: *A constant vorticity trajectory differential analyser* (unpublished), 8 pp.